STUDIA UBB CHEMIA, LXX, 4, 2025 (p. 107-129)
(RECOMMENDED CITATION)
DOI:10.24193/subbchem.2025.4.07

WASTE GRAPE POMACE FOR FOOD PACKAGING

Daniel BOMBOȘ[a], Gabriel VASILIEVICI[b,*], Ana Maria MANTA[c], Loredana Irena NEGOIȚĂ[c], Ioan SAROSI[d], Andrei MOLDOVAN[d], Filip MIUTA[e], Andra-Ioana STĂNICĂ[f], Stanca CUC[e]

ABSTRACT. The use of waste wine byproducts in packaging manufacture can offer an alternative to plastic pollution. Thus, grape pomace possesses properties that could improve the performance of plastic materials. In this work, the conditioning of grape pomace was studied for the purpose of adding PLA films. Resveratrol was extracted from grape pomace, which was then incorporated into PLA films to enhance their performance. The obtained biopolymers were characterized by determining the mechanical, thermal, and structural properties. The tensile strength of the composites has similar values for the composite with pomace and those with resveratrol, and a similar flexibility of the analyzed samples. The thermal stability of the pomace waste and the composites to which pomace and resveratrol were added was high. DSC tests of PLA-based composites revealed two endothermic peaks at temperatures above 120 °C, probably caused by the melting of amorphous structures. Surface examination indicated a relatively uniform distribution of pomace or resveratrol particles in the polymer matrix, and surface roughness parameters calculated by atomic force microscopy indicated a low to moderate level of roughness, with higher values for pomace-containing films than for resveratrol-based ones, highlighting the more hydrophilic nature of pomace-containing films compared to resveratrol-based ones.

Keywords: *grape pomace, resveratrol, biopolymer, PLA composite*

[a] *S.C. Medacril S.R.L, 8 Carpați Street, Mediaş, Sibiu County, Romania*
[b] *National Institute for Research Development for Chemistry and Petrochemistry-ICECHIM-Bucharest, 202 Spl. Independenței, 060021 Bucharest, Romania*
[c] *Petroleum-Gas University of Ploieşti,39 București Blvd.,100680, Ploieşti, Romania*
[d] *Department Environmental Engineering and Sustainable Development Entrepreneurship, Technical University of Cluj-Napoca, 400641 Cluj-Napoca, Romania*
[e] *Institute of Chemistry "Raluca Ripan", Babes-Bolyai University, 30 Fântanele Street, 400294 Cluj-Napoca, Romania*
[f] *Technological High School "Toma Socolescu", Gheorghe Grigore Cantacuzino St., 328, 100466, Ploiești, Romania*
* *Corresponding author: gvasilievici@icechim.ro*

INTRODUCTION

Grape pomace, one of the main by-products of winemaking, describes approximately 20% of the total mass of processed grapes; it is a complex product composed of polysaccharides, pectins, phenolic compounds, lignin, structural proteins and phenols [1]. Thus, it has been highlighted that grape pomace contains bioactive compounds that can be obtained along with other value-added products, to bring socio-economic and environmental benefits [2-3].

The field of nanotechnology reveals innovative solutions for waste valorisation through the synthesis of nanomaterials with special chemical and physical properties, making them suitable for numerous applications, including safety protocols and environmental monitoring [4-8].

Directing bio-wastes on new pathways to usable products or raw materials has gained a lot of popularity [9-12]. In recent years, there has been great development underway to improve bio-waste transformation processes to generate different raw materials, especially for bioplastic production [13]. Thriving use of renewable resources will not only help changeover to the circular economy but will also lead to significant ecological advantages such as decreasing greenhouse gas emissions, reducing the volume of harmful pollutants, and protecting ecosystems and biodiversity [14-17].

According to previous studies, the winemaking by-products contain a significant number of fatty acids and phenolic compounds with viable applications in the food industry [18]. Pomace has been partially valorised by now, mainly for oil extraction from the grape seeds in view of utilising it in the pharmaceutical industry for its antioxidant and antibacterial properties [19].

In addition, sustainable food packaging materials have been developed from polyphenols and associated fibre extracted from pomace. The use of these active extracts in the development of biodegradable active packaging materials serves as a striking substitute for food preservation, adding value to bioplastics by enhancing their functionality [20-22]. The food packaging materials have to protect food against UV light and should also be supplemented with probiotics, a class of microorganisms with great importance for the digestive system, which can improve digestion when they reach the stomach along with the packed food [23-24].

The increased consumer demand for fresh and natural foods comes along with innovative concepts of smart food packaging with an extended shelf life, competitive price and greater accessibility during storage and transportation [25]. Antimicrobial agents impregnated on packaging materials can slowly diffuse onto the food surface to combat food-borne microorganisms [26]. The grape skin cell wall contains cellulose, hemicellulose, pectin, and lignin, which

form a complex structure, while the main components of grape seeds are cellulose and pectin. Cellulose Nano Crystals (CNCs) are the best options for the development of nano-composite materials, due to their high crystallinity and large surface area, which are important properties for high-performing composites [27]. These active compounds can be extracted by various methods, such as ultrasound, high interest in using environmentally friendly solvents, like subcritical water, instead of conventional organic solvents. The efficiency and selectivity of the process depend on the state parameters, water-increasing temperature being the most important factor, which reduces the dielectric constant and the polarity of water molecules, thus enhancing the dissolution of less polar compounds in water [28].

Polysaccharide films investigated for food packaging have a good oxygen barrier, but their humidity resistance is weaker. A solution to this problem is bilayer films made by crosslinking and PLA addition. Cellulosic multilayer films proved to offer a good barrier for oil and gas, although they require chemical modification through esterification or etherification processes. The results demonstrate that multi-layer structures of PLA, fully biodegradable by natural microorganisms such as bacteria and fungi, can be designed with the aim of enhancing performance in food packaging [29].

Among the available biobased polymers, there is polybutylene succinate (PBS), which has convenient mechanical properties in comparison to petrochemical polymers such as polyethylene or polypropylene. The main inconvenience to PBS is its tendency to degrade by thermo-oxidative mechanisms. To prevent unwanted degradation processes, there comes the need to stabilize the polymers by adding functional stabilizers. Resveratrol, another important component of the grape seeds, has also proven to be able to slow the oxidative chain reaction of polymers through a peroxyl radical scavenging mechanism, while it has little effect on the direct photolytic cleavage of the ester bonds [30-31].

The food packaging industry is expected to grow, as the use of waste such as wine by-products minimizes food waste and offers an alternative to plastic pollution, with a negative impact on the environment. Grape pomace possesses favorable properties for the addition of plastics and, through physical processes such as extraction or chemical processes such as maceration, active principles can be obtained that can contribute to improving the performance of biopolymers to obtain valuable packaging materials with favorable mechanical properties, flexibility, as well as improved antibacterial activity. This work addresses the valorization of grape pomace in order to obtain active food packaging based on polylactic acid (PLA). The pomace waste was conditioned in powder form or was recovered by extracting a concentrated fraction of resveratrol. The two additives, namely pomace and

resveratrol, were characterized and used in the preparation of PLA-based composites, which were characterized by determining the mechanical, thermal, and microstructural characteristics.

RESULTS AND DISCUSSION

Characterization of grape pomace

Scanning Electron Microscopy (SEM)

From the SEM images, bundles with a fibrous structure, under 100 µm, with numerous holes formed as a result of the entanglement of the fibers are observed (figure 1).

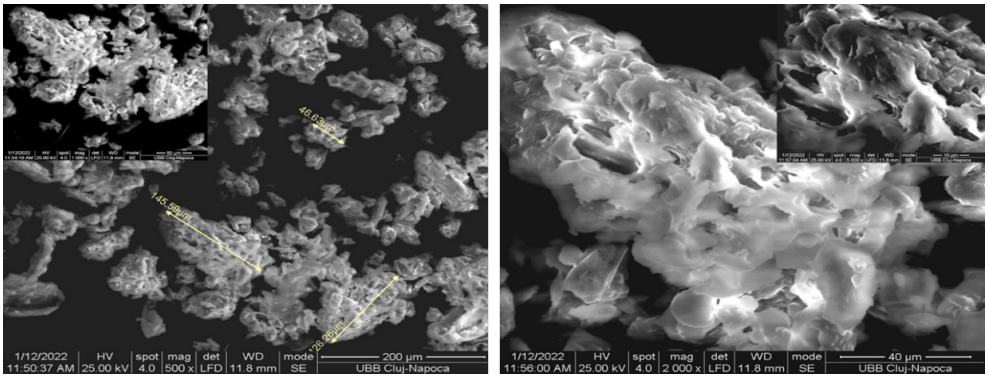

Figure 1. SEM images of grape pomace powder

Thermogravimetric Analysis (TGA)

The thermal decomposition of PLA Cu samples is depicted in Figure 2. Three important areas are observed. (1) The first one is an area with a mass loss of up to 6.45% by weight, the area located at temperatures of up to approximately 225^{o}C. (2) The second one is an area with a mass loss of up to 16.90% by weight, the area located at temperatures of 225-325^{o}C. (3) The last one is an area with a mass loss of up to 63.60% by weight, the area located at temperatures of 325-500oC. Mass losses for the first two zones are due to the evaporation of water and compounds with different volatilities, such as polyphenols, carboxylic acids, etc., and for the third zone, they are due to the thermal decomposition processes of hardly volatile compounds such as carbohydrates, lignin, resveratrol etc.

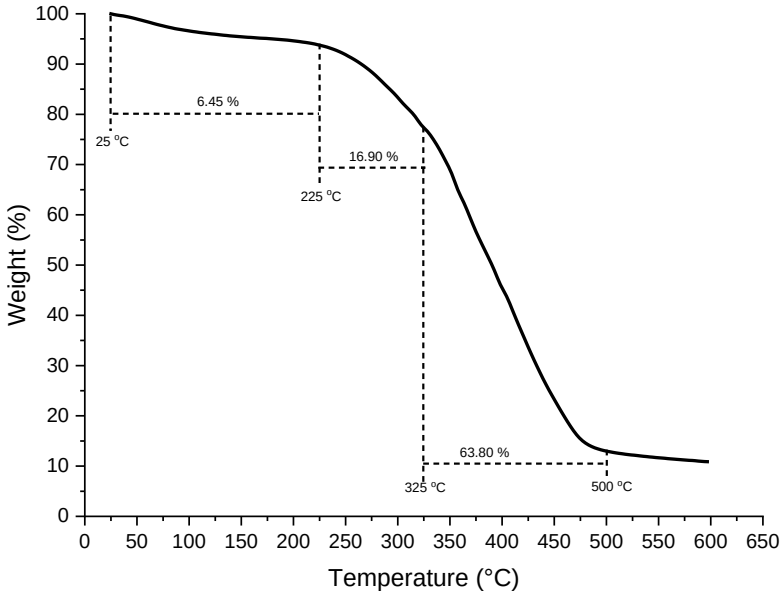

Figure 2. Thermogravimetric analysis (TGA) for grape pomace

Characterization of resveratrol

SEM analysis

Resveratrol powder particles have geometric or irregular shapes, with flat, shiny surfaces and sharp edges, on which deposits of much smaller powder particles can be noticed (Figure 3). Most cylindrical particles have lengths below 100 µm.

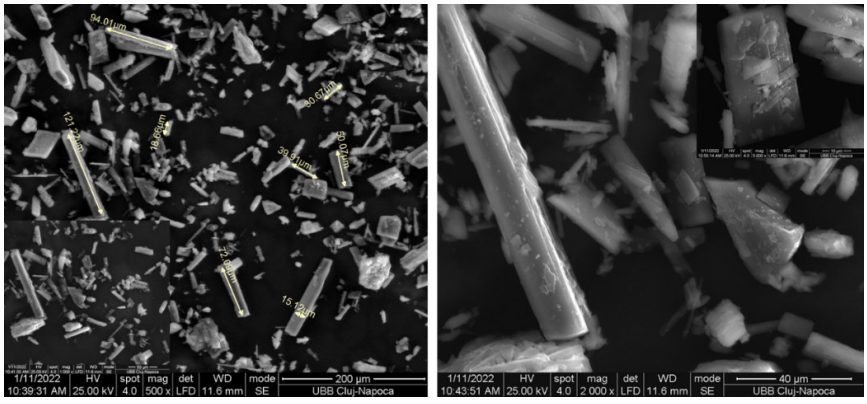

Figure 3. SEM images of resveratrol

HPLC analysis

The HPLC chromatogram of the resveratrol extract after concentration and the resveratrol standard are shown in Figures 4 and 5. The HPLC chromatograms show the presence of a relatively small number of components in the concentrated resveratrol extract. Based on this analysis, the efficiency of the purification process of the concentrated resveratrol extract can be highlighted, considering the large number of components present in such products.

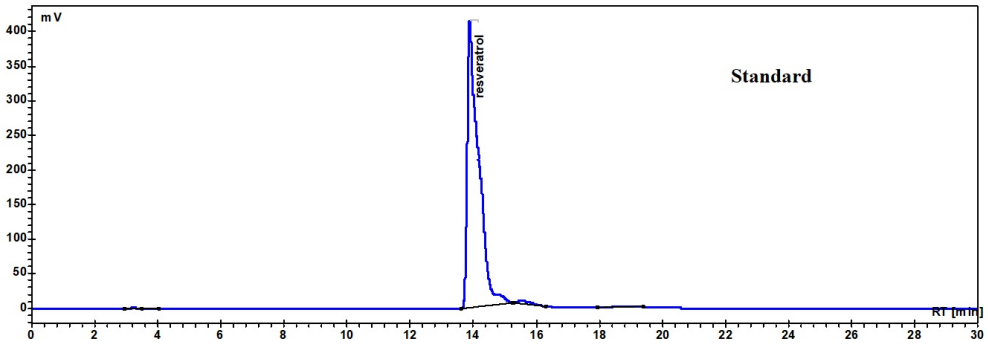

Figure 4. HPLC chromatogram of the resveratrol standard.

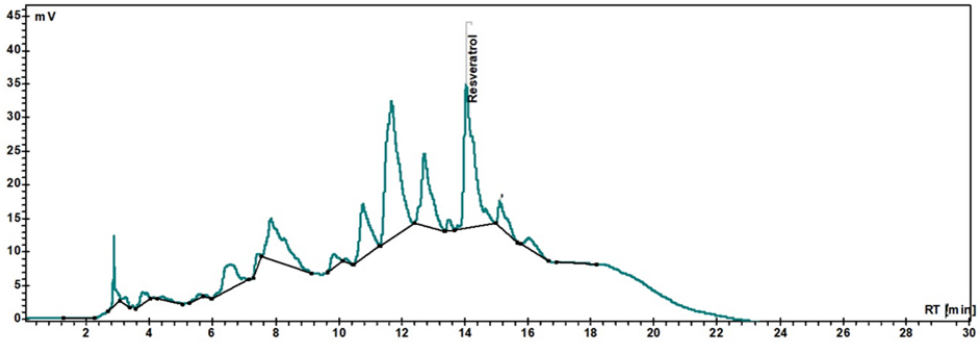

Figure 5. HPLC chromatogram of concentrated resveratrol extract

FTIR analysis of grape pomace

In Figure 6, the asymmetric and symmetric stretching vibrations of the CH_2 groups are observed at 2919 and 2852 cm^{-1}, respectively. These are mainly associated with the hydrocarbon chains of lipids or lignins as noted

by Lucarini et al. [33]. The spectral band at 1741 cm^{-1} is attributed to the absorption of the C=O bonds of ester groups and is related to the presence of fatty acids and their glycerides, as well as pectins and lignins as noted by Gao et al. [34]. The fingerprint region from 1500 to 800 cm^{-1} is very rich in peaks originating from different stretching, bending, rocking, shearing and torsion modes. This region is, on the one hand, very rich in information, but, on the other hand, difficult to analyze due to its complexity. This region provides important information about the organic compounds, such as sugars, alcohols and organic acids, present in the sample. The aliphatic C-O stretch at 1261 cm^{-1} is related to alcohols. The aromatic C-H stretch at 1143 cm^{-1} can be attributed to phenolic compounds. The O-C-C stretch at 1457 cm^{-1} indicate the presence of the phenolic compounds as noted by Heredia-Guerrero et al. [35]. The out-of-plane CH_3 bending at 1064 cm^{-1} is related to polysaccharide structures as noted by Gao et al. [34]. The band at 788 cm^{-1} is due to the CH_2 swing of phenolic compounds as noted by Lucarini et al. [32].

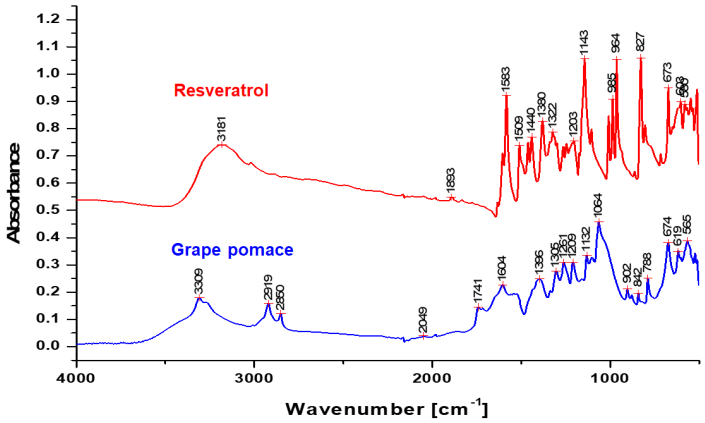

Figure 6. FT-IR spectra of grape pomace and resveratrol

Characterization of synthesized recipes

The prepared PLA films were homogeneous, opaque, faintly colored, and did not contain embedded air bubbles.

Tensile test results

As can be seen in Table 1, the tensile strength of the composites has similar values for the composites with pomace and those with resveratrol. Young's modulus has higher values for the composites with pomace and the breaking elongation has higher values for the composites with resveratrol.

Table 1. Tensile test results

Sample Code	Tensile strength (MPa)	Maximum load (N)	Breaking Strength (N)	Breaking Elongation (mm)	Young's modulus (MPa)	Breaking Stress (MPa)
PT1	16.31±2.84	157.97±51.77	159.69	34.290	556.11	15.01
PT 2	15.45±5.97	159.69±38.26	159.69	23.600	532.22	13.38
PT3	18.726±4.68	189.29±50.21	181.60	54.356	593.68	15.98
PR1	19.40±6.84	194.88±49.15	194.88	103.78	126.71	19.40
PR2	25.99±6.87	237.89±47.56	237.89	127.14	15.23	25.96
PR3	19.38±4.33	201.54±45.85	201.54	118.28	11.42	19.28
p-value	*	**	**	***	***	**

* first relevant statistic group ($p < 0.05$) ** second relevant statistical group ($p < 0.05$)
*** the third statistical relevant group ($p < 0.05$)

Flexural Strength Testing

The results obtained for the three-point bending tests are depicted in Table 2. From the investigation of the bending tests it is observed that the flexibility of the samples presents close values for all the analyzed samples. The Young's modulus of the samples is directly proportional to the maximum force supported and is inversely proportional to the elongation and decreases with increasing additive concentration.

Table 2. The obtained results for three points Flexural Tests

Sample Code	Maximum Load (N)	Young Modulus (MPa)	Bending Stiffness (Nm^2)	Maximum Bending Stress at Maximum Load (MPa)	Elongation (mm)
PT1	44.24±4.14	214.7690±40.16	0.0044	22.45±2.85	9.22±1.01
PT 2	40.48±0.57	196.24±16.72	0.0047	19.07±1.33	9.12±0.6
PT3	12.49±4.08	105.02±58.44	0.0030	5.50±1.95	8.86±0.5
PR1	5.02±2.70	383.31±1.79	0.0016	2.12±0.58	5.56±1.57
PR2	12.33±1.44	155.96±50.86	0.0029	6.72±0.53	8.74±0.34
PR3	42.48±1.23	59.17±40.92	0.0066	22.16±1.32	9.79±0.46
p-value	**	***	*	**	*

* first relevant statistic group ($p < 0.05$) ** second relevant statistical group ($p < 0.05$)
*** the third statistical relevant group ($p < 0.05$)

The elongation value did not change significantly with the content of pomace or resveratrol, probably due to the mobility induced by the nature of the plasticizer used in the experiments.

Thermogravimetric analysis

The behavior of PLA films added with grape pomace is illustrated in Figure 7 through TG curves and in Figure 8 through DTG curves. For the three composites it is observed that the mass losses are insignificant at temperature values lower than 300 ºC and are due to the vaporization of the more volatile components present in the pomace or plasticizer. These mass losses become significant at temperatures above 300 ºC and are due to the homolytic dissociations of the C-O and C-C bonds in the plasticizer and polyester molecules. The mass losses decrease at temperatures of almost 380 ºC. The cracking residue at temperatures above 400 ºC has relatively low values (tends to zero).

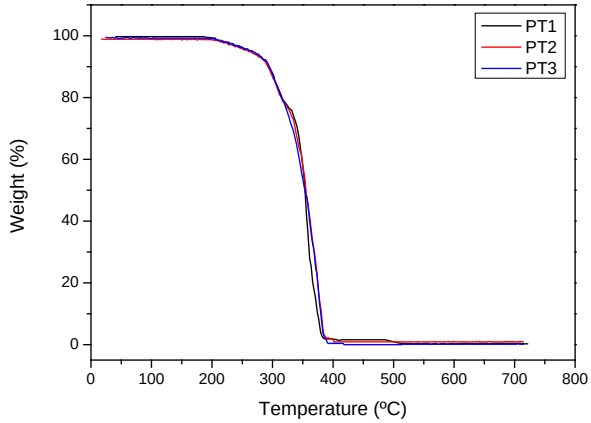

Figure 7. TGA curve for grape pomace-based composites

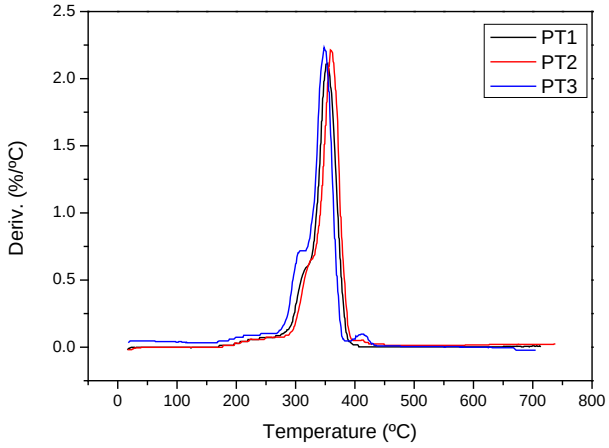

Figure 8. DTG curve for grape pomace-based composites

The thermal stability of PLA composite containing 0.5 to 1.5 wt.% resveratrol is illustrated in Figures 9 and 10. Both the TG and DTG curves show that the three resveratrol-based composites exhibit similar thermal stability to the pomace-based composites.

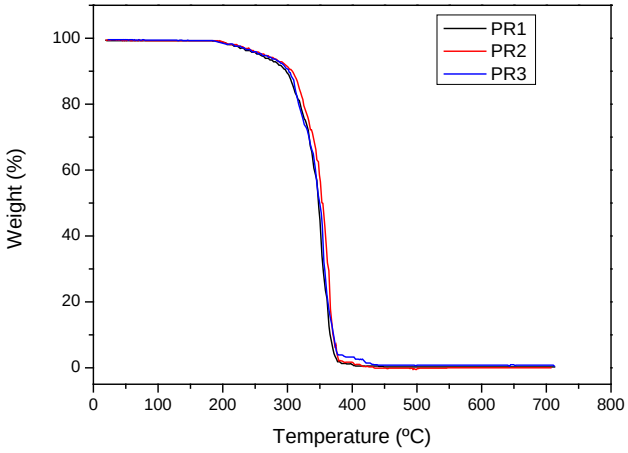

Figure 9. TGA curve for resveratrol-based composites

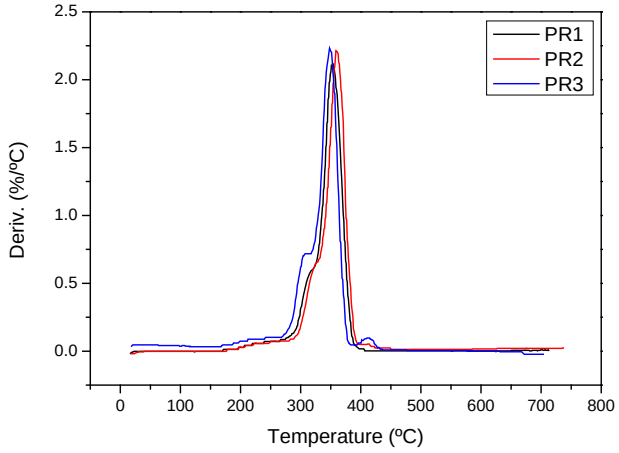

Figure 10. DTG curve for resveratrol-based composites

DSC analysis

The influence of grape pomace and resveratrol on the thermal transitions of PLA composites is shown in DSC thermograms Figure 11 and in Table 3. As can be seen, the addition of pomace to PLA induced the appearance of two endothermic transformations located at temperature values higher than 120 °C. Also, over the temperature range studied, the transition from the glassy state to the thermoplastic state was not identified, Tg therefore having values lower than 25 °C. This behavior is attributed to the improvement of PLA mobility due to the characteristics of the plasticizer that enhance the decrease of the glass transition temperature, regardless of the pomace concentration value. In the case of samples to which resveratrol was added, a similar behavior was observed, with two endothermic peaks being evident at temperatures above 120 °C, probably caused by the melting of amorphous structures, the size of the peaks being proportional to their concentration.

Table 3. Characteristic temperatures for PLA films added with pomace and resveratrol

Sample	Quantity (mg)	DSC		The process type
		Temperature interval (°C)	Temperature transformation (°C)	
PT1	13.9020	25-135	Onset 119 132	endothermic process
		135-200	145	endothermic process
PT2	13.9380	25-135	Onset 121 133	endothermic process
		135-200	146	endothermic process
PT3	10.3000	25-135	Onset 122 131	endothermic process
		135-200	146	endothermic process
PR1	16.0600	25-135	Onset 124 132	endothermic process
		135-200	146	endothermic process
PR2	11.4540	25-135	Onset 118 131	endothermic process
		135-200	146	endothermic process
PR3	13.8850	25-135	Onset 121 131	endothermic process
		135-200	146	endothermic process

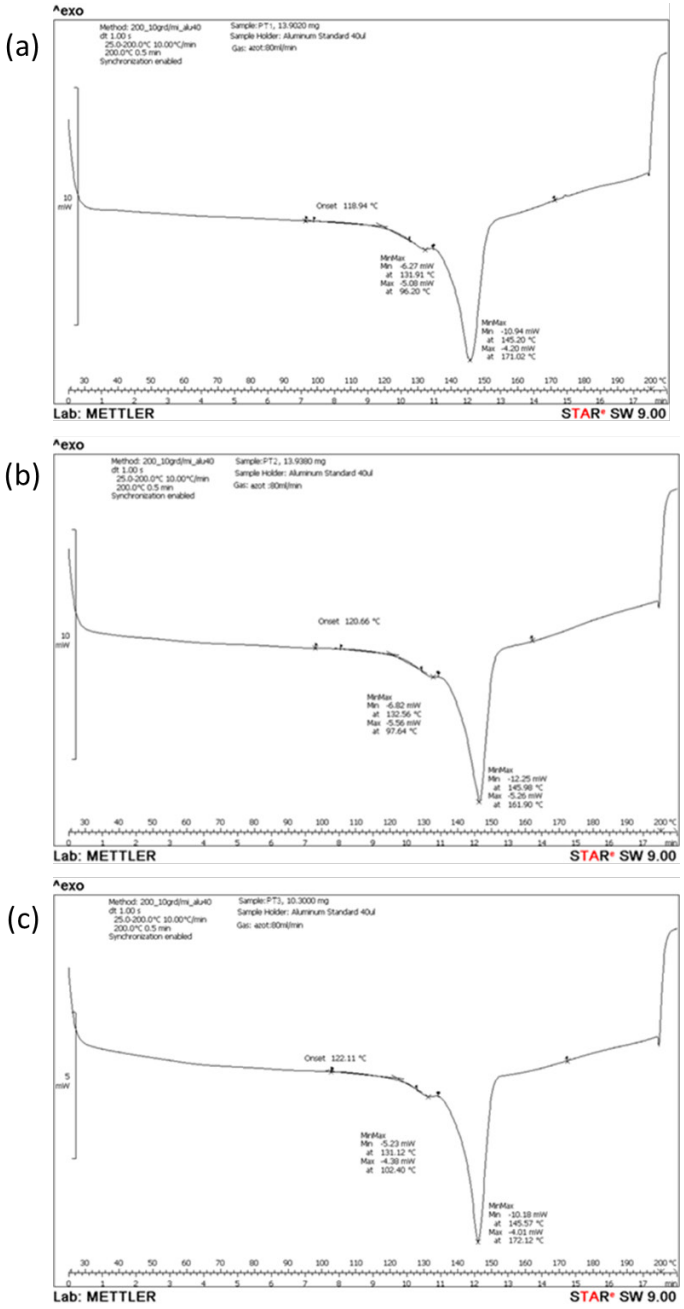

Figure 11. DSC curve for: (a) PT1 composite, (b) PT2 composite, (c) PT3 composite.

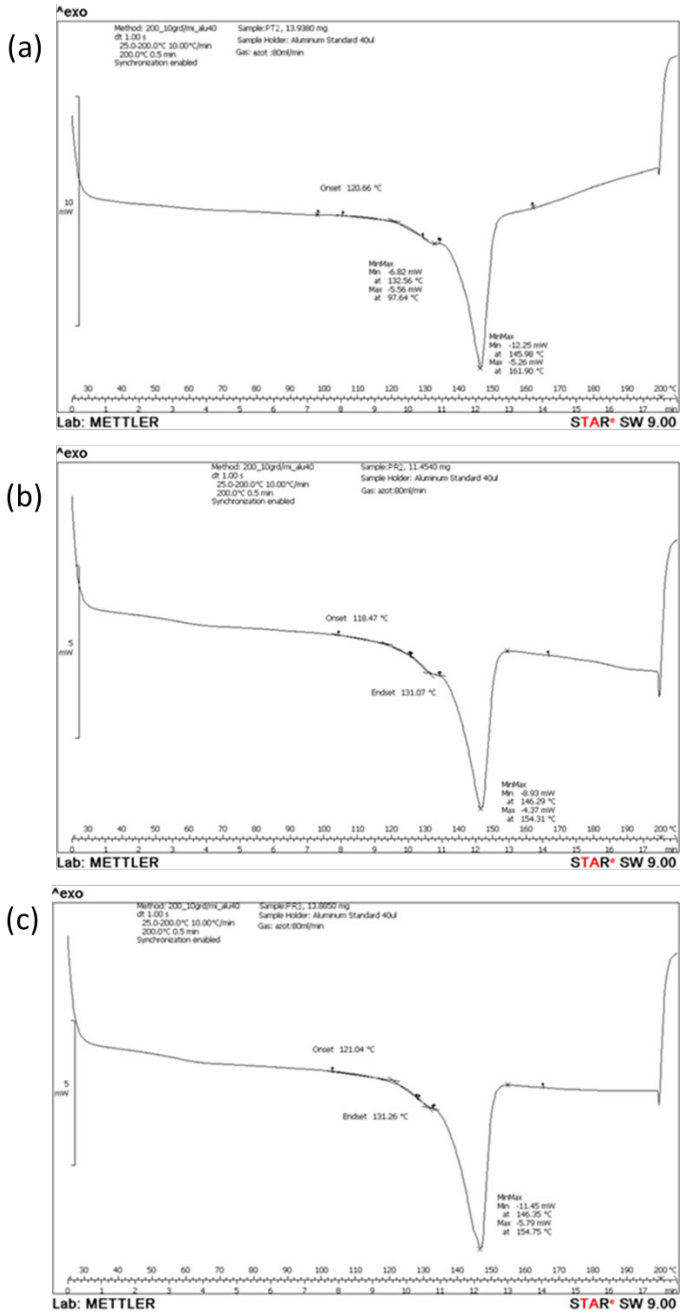

Figure 12. DSC curve for: (a) PR1 composite; (b)PR2 composite; (c) PR3 composite.

Scanning electron microscopy (SEM) analysis

Scanning electron microscopy analysis of PLA films doped with pomace or resveratrol (PT1-3 and PR1-3), performed at 2000 magnifications (40 µm) (Figures 13), reveals a relatively uniform distribution of pomace or resveratrol particles in the polymer matrix, probably facilitated by the close polarity of the plasticizer with the two additives. The presence of additive microclusters is observed in all samples, especially at higher resolutions. Increasing the additive concentration determined the increase in the size of the microclusters, a more obvious increase in the case of the PLA film doped with pomace. In conclusion, the SEM micrographs demonstrate that the incorporation of the two additives into the PLA matrix was successful, with minimal surface defects, which makes the material potentially suitable for packaging applications.

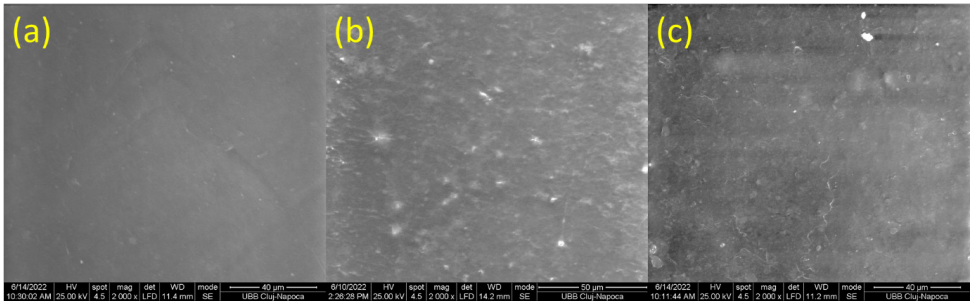

Figure 13. SEM micrographs of: (a) PT1; (b) PT2; (c) PT3 sample at 2000 magnifications.

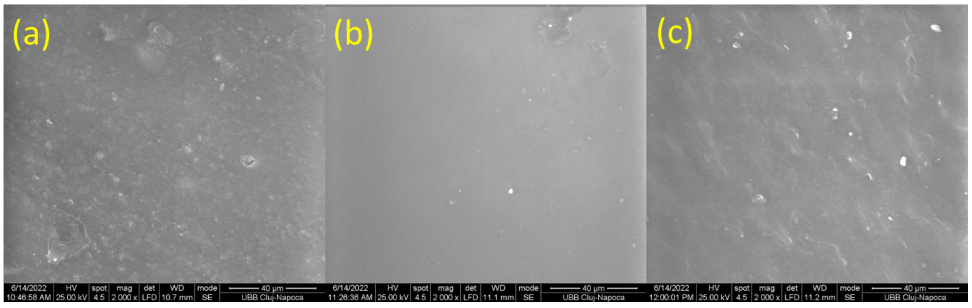

Figure 14. SEM micrographs of: (a) PR1; (b) PR2; (c) PR3 sample at 2000 magnifications.

Atomic force microscopy (AFM) analysis

Analysis of the surface of PLA-based films, previously stored in saline solution, by atomic force microscopy (AFM) provided a more detailed picture of the microstructural units and their topographical characteristics.

The analysis of the PLA film surface by atomic force microscopy provided more detailed images of the microstructural units, as well as the topographical features. Both the advanced dispersion of the pomace (Figure 15) and resveratrol nanoparticles (Figure 16), but also variations in the film thickness are highlighted. The topographical image reveals clusters of pomace or resveratrol, with a more or less uniform distribution, suggesting a relatively good compatibility between the PLA matrix and the two additives. The three-dimensional profile of the film surface highlights a texture whose homogeneity decreases with increasing pomace or resveratrol content. The calculated surface roughness parameters, an average roughness (Ra) and a root mean square roughness (Rq) at a low to moderate roughness level, with higher values for the films containing pomace than for those based on resveratrol and increasing with the additive content. This behavior is due to a higher water absorption in the pomace-based PLA film, probably due to its more hydrophilic character compared to resveratrol.

Literature data reveal that the proper dispersing of the filler particles ensures an optimal cohesion within the composite material [36, 37]. The mineral filler (e.g., such a small micro fraction) dispersion is very susceptible to the fluidity of the dispersion environment [38]. Mugnaini et al. reveal that the grape pomace addition into the composite material causes a relative increase of the surface roughness from about 40 nm up to 60 nm due to the enhancing of the hydrophilic behavior that interacts with the cantilever's tip [39]. Similar behavior is observed by de Souza Cohelo et al. [40]. Thus, the initial fluidity of the composite material plays an important role in the even particle distribution, which is kept after polymerization.

Furthermore, a smooth and uniform surface has a small roughness as observed by Atomic Force Microscopy [41] and the composite materials' roughness strongly depends on the filler particles reaching the outermost layers [42,43]. The initial well-done lamination of the filler particles keeps the surface roughness as low as possible. Literature reveal that the lateral pressure [44] associated with any liquid penetration might cause delamination of the outermost filler particles increasing the surface roughness. Resveratrol has spreading into the composite nanostructure increases the surface roughness in a pronounced manner via local hydrophilicity associated with highly negative charged surface as observed by Tan et al. [45]. The roughness increase is caused by the increasing of contact angle from 88.2 ± 4.58˚ to

about 115.54 ± 1.12˚ induced by resveratrol (Brahamian et al.) making the composite ideal for proactive food packaging. [46] The proactive role of the relative increased roughness under bioactive behavior of resveratrol filled composites is also confirmed by Wu et al. [47]. The local heights of the gelatin–resveratrol increase from about 20 nm to about 40 nm as consequence of its uniform distribution within the matrix (Fu et al.) [48].

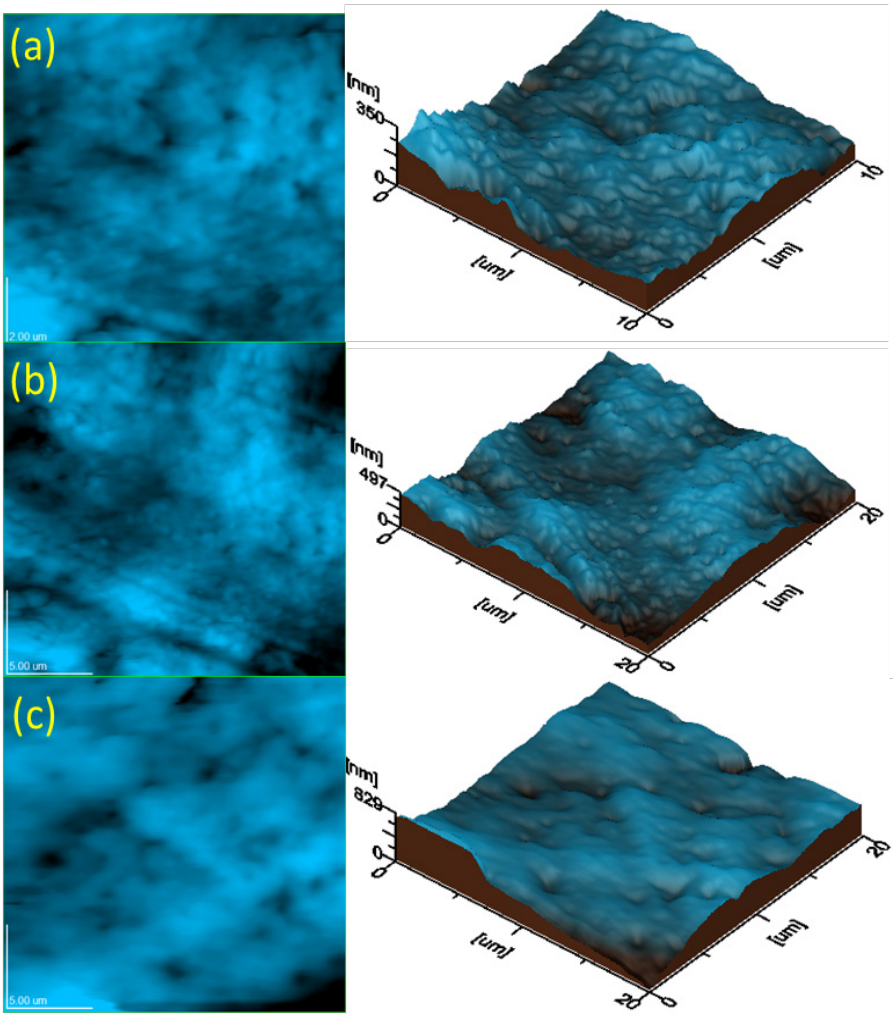

Figure 15. Topographic characteristics of: (a) PT1 - scanned area 10 µm x 10 µm, Ra area 31.6 nm; Rq area 40.5 nm; (b) PT2 - scanned area 20 µm x 20 µm, Ra area 63.6 nm; Rq area 78.5 nm; (c) PT3 - scanned area 20 µm x 20 µm, Ra area 61.5 nm; Rq area 85.0 nm.

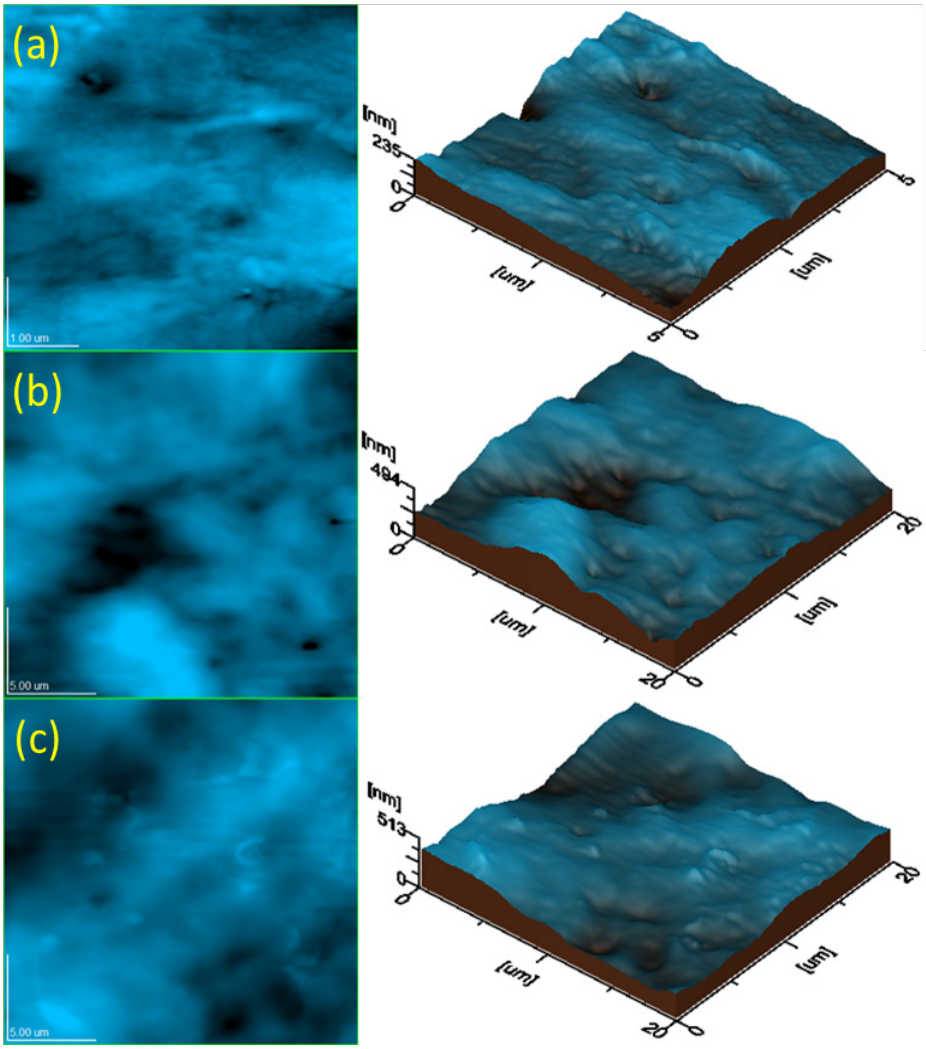

Figure 16. Topographic characteristics of: (a) PR1 - scanned area 5 µm x 5 µm, Ra area 21.4 nm; Rq area 27.1 nm; (b) PR2 sample - scanned area 20 µm x 20 µm, Ra area 47.5 nm; Rq area 61.3 nm; (c) PR3 - scanned area 20 µm x 20 µm, Ra area 56.6 nm; Rq area 68.1 nm.

The limitations of the current study are generated by the low concentrations of the powdered additive (below 1.5%), either due to the color change of the PLA film favored by the pomace, or due to the high price of resveratrol.

Future research directions consider optimizing the composition of the plasticizer mixture in order to improve the film elongation and performing bacteriological studies of the optimized formulations.

CONCLUSIONS

Grape pomace waste was conditioned in powder form or was recovered by extracting a concentrated fraction of resveratrol. The two additives, respectively pomace and resveratrol, were characterized and used in the preparation of PLA-based composites that were characterized by determining the mechanical, thermal and microstructural characteristics. The tensile strength of the composites has similar values for the composites with pomace and those with resveratrol, with Young's modulus having higher values for the composites with pomace. Bending tests revealed a similar flexibility of the analyzed samples and values of Young's modulus directly proportional to the maximum force supported. The thermal stability of the grape pomace waste and the composites added with pomace and resveratrol obtained was evaluated by thermogravimetric analysis, highlighting their good thermal stability. DSC tests of PLA-based composites revealed two endothermic peaks at temperatures above 120 °C. The melting of the amorphous structures, the size of the peaks being proportional to their concentration probably cause these. The mobility of PLA macromolecules induced by the plasticizer tributyl 2-acetylcitrate favored the decrease of Tg and the obtaining of an elongation of applicative interest for the two types of composites studied. Surface examination indicated a relatively uniform distribution of pomace or resveratrol particles in the polymer matrix with small micro-clusters of additive aggregates, especially in composites where the additive concentration is higher. Surface roughness parameters calculated by atomic force microscopy indicated a mean roughness (Ra) and root mean square roughness (Rq) at a low to moderate roughness level, with higher values for pomace-containing films than for resveratrol-based ones, highlighting the more hydrophilic nature of pomace-containing films compared to resveratrol-based ones.

EXPERIMENTAL SECTION

Materials and Methods

Polylactic acid (PLA, Ingeo® brand, NatureWorks LLC, Tokyo, Japan), Proviplast® 2624 by Proviron (tributyl 2-acetylcitrate), chloroform, methanol and

ethyl acetate from Aldrich-Sigma (Schnelldorf, Germany). In this study, grape pomace was from the grape variety “Vitis” interspecific crossing “Noah”, family Vitaceae.

Preparation of the Biomass

The pomace was washed in three stages with distilled water at a mass ratio of water/pomace 10/1, then dried in an oven at 60 °C for 24 hours and cut into smaller pieces. The resulting dried pomace was finely ground with a GRINDOMIX GM 200 knife mill, manufactured by Retsch GmbH, and sieved to a powder with a particle size ≤ 200 μm.

Resveratrol was obtained from grape pomace according to the procedure described by Trifoi A. et al. [32]. Thus, we macerated 100 g of dried and ground grape pomace in 1000 ml of methanol at room temperature for 24 h, after which the mixture was subjected to a reflux extraction process for 60 min., under continuous stirring, at a rotation of 400 rpm. After reflux extraction, the mixture was filtered and the extract solution was concentrated under vacuum, then dispersed in water adjusted to pH 1 with hydrochloric acid, at an extract: water ratio of 1:10 and subjected to the hydrolysis process for 20 h, at 60°C. To recover resveratrol from the hydrolyzed aqueous solution. The aqueous solution of resveratrol was subjected to a three-stage liquid-liquid extraction process in a separatory funnel in the presence of ethyl acetate at a volumetric ratio of 1/1. Then the extract was decolorized with TONSIL bleaching earth, and the resveratrol was recovered by precipitation in water and filtered.

Preparation of PLA-based films

The solubilization of polylactic acid (PLA) was carried out at a controlled temperature of 50°C, using a stirring speed of 500 rpm. After complete dissolution of PLA, the plasticizer and then the additive (pomace or resveratrol powder) were successively added to the solution. The resulting homogeneous mixture was then poured into sterile Petri dishes for solvent evaporation to form the film. Three active formulations based on powdered pomace and three active formulations based on resveratrol were prepared, as shown in Table 4.

Table 4. Composition of PLA-based films

Sample no.	Polylactic Acid (% w/w)	Proviplast 2624 (% w/w)	Grape pomace (% w/w)	Resveratrol (% w/w)
PT1	79,5	20,0	0,5	-
PT2	79,0	20,0	1,0	-
PT3	78,5	20,0	1,5	-
PR1	79,5	20,0	-	0,5
PR2	79,0	20,0	-	1,0
PR1	78,5	20,0	-	1,5

Biomass and PLA composite characterization

The obtained pomace powder was analyzed by SEM microscopy, FTIR analysis and TGA. Resveratrol was analyzed by SEM microscopy and by HPLC chromatography. To evaluate the physicochemical characteristics of the developed PLA-based composite films, mechanical thermal, and surface analyses were performed using state-of-the-art techniques. These characterizations aimed to evaluate the impact of pomace and resveratrol additives on the performance of the films.

HPLC analyses were performed on a Jasco HPLC chromatograph (Japan) equipped with an HPLC pump (Model PU-980), a ternary gradient unit (Model LG-980-02), a column thermostat, a UV-Vis detector (Model UV-975), and an injection valve equipped with a 20 µL sample loop (Rheodyne). Samples were manually injected with a Hamilton Rheodyne syringe (50 ml). The HPLC system was controlled and the experimental data were analyzed with ChromPass software.

The microstructural characteristics of the samples were determined using scanning electron microscopy (SEM) and atomic force microscopy (AFM). SEM images were acquired using an Inspect S- SEM microscope (FEI, Hillsboro, OR, USA) operated under high vacuum at an accelerating voltage of 30 kV. This method enabled detailed visualization of the dispersion of fillers, phase separation, and surface homogeneity. The surface topography of the samples was investigated by scanning Atomic Force Microscopy (AFM) performed with a JEOL JSPM 4210 device, produced by JEOL, Japan, Tokyo. Fourier Transform Infrared Spectroscopy (FTIR): was employed to investigate the molecular structure and the specific functional groups present in the pomace.

Fourier transform infrared (FT-IR) spectra were recorded on a Spectrum BX (Perkin Elmer, Waltham, MA, USA) FTIR spectrometer, equipped with an ATR accessory (PIKE MIRacleTM), with a diamond crystal plate in attenuated total reflection (ATR) mode.

Thermogravimetric analysis assessed the thermal stability of biomass and biochar using the thermogravimetric/derivative apparatus TGA/DTG (TGA 2 Star System Mettler Toledo, Zurich, Switzerland). Differential Scanning Calorimetry (DSC) was carried out with the help of a 630e, 700C Mettler-Toledo calorimeter (Switzerland). Measurement conditions: aluminum crucible-40 µL; heating speed: 10 oC/min; temperature range 25–200 oC; final landing 0.5 min; atmosphere: nitrogen; flow rate: 80 mL/min.

The rectangular specimens specific to this test were subjected to tensile tests using the Lloyd LR5k Plus universal mechanical testing machine (Lloyd Instrumente, Ametekln s, West Sussex, England), with a maximum allowed capacity of 5KN, at a loading force of 0.5 N and a speed of 1 mm/minute at ambient temperature (25 ^{o}C), according to the ASTM D638-14, using

Nexygen software (version 4.0). The flexural strength was achieved by the 3-point technique, according to ASTM D 790; the data were processed using the Nexygen software (version 4.0). All the data are the average of at least seven measurements. The statistical differences between the groups of investigated samples were statistically analyzed using the one-way ANOVA test.

ACKNOWLEDGMENTS

"Development of innovative food packaging without negative impact on the environment (AMBAL-INOV)", My SMIS: 120994, contract: 375/ 390051/ 30.09.2021, Competition: 63/POC/163/1/3/LDR.

REFERENCES

1. E.T. Nerantzis, P. Tataridis, *E-J. Sci. Technol.,* **2006**, *1*, 79–89. 32 Handbook of Grape Processing By-Products
2. N. Jimenez-Moreno, I. Esparza, F. Bimbela, L.M. Gandía, C. Ancín-Azpilicueta, **2020**, *50(20),* 2061–2108. https://doi.org/10.1080/10643389.2019.1694819
3. N. P. Nirmal, A. C. Khanashyam, A. S. Mundanat, K. Shah, K. S. Babu, P. Thorakkattu, et al., *Foods*, **2023**, *12(3)*, 556, https://doi.org/10.3390/foods12030556
4. M. Primozic, Z. Knez, M. Leitgeb, M., *Nanomaterials*, **2021**, *11(2)*, 1–31. https://doi.org/10.3390/nano11020292 MDPI AG
5. M. Sanda, I. Onuțu, C. M. Dușescu-Vasile, G.Vasilievici, D. Bomboș, M. Băjan, G. Brănoiu, *Molecules*, **2025**, *30 (9),* 1962, https://doi.org/10.3390/molecules30091962
6. D. Popovici, C. Duşescu, M. Neagu, *Revista de Chimie*, **2016**, *67(4),* 751-756
7. M. Neagu, D.R. Popovici, C. M. Duşescu, C. Calin, *Revista de Chimie,* **2017**, 68(1), 139-142
8. D.R. Popovici, M. Neagu, C.M. Dușescu-Vasile, D. Bombos, S. Mihai, E.E. Oprescu, *Reaction Kinetics, Mechanisms and Catalysis*, **2021**, *133 (1),* 483-500
9. C. Duşescu, I. Bolocan, *Revista de Chimie*, **2012**, *63*(3), 305-309
10. C. Duşescu, I. Bolocan, *Revista de Chimie*, **2012**, 63(7), 732-738
11. C. Duşescu, P. Roşca, D. Bombos, T. Jugãnaru, D. Popovici, R. Dragomir, *Revista de Chimie*, **2012**, *63(2),* 229-231
12. V Gheorghe, C.G. Gheorghe, A. Bondarev, V. Matei, M. Bombos, *Revista de Chimie,* **2019**, *70(8)*, 2996-2999
13. M. Carmona-Cabello, I.L. Garcia, D. Leiva-Candia, M.P. Dorado, *Curr. Opin. Green Sustain. Chem*. **2018**, *14*, 67-79. https://doi.org/10.1016/j.cogsc.2018.06.011 2018
14. O. V. Săpunaru, A.E. Sterpu, C. A. Vodounon, J. Nasr, C. Duşescu-Vasile, S. Osman, C I. Koncsag, *Lubricants*, **2024**, *12*(6), 197, https://doi.org/10.3390/lubricants12060197

15. R. Shogren, D. Wood, W. Orts, G. Glenn, *Sustain. Prod. Consum*., **2019**, *19*, 194–215. https://doi.org/10.1016/j.spc.2019.04.007
16. S. Viswanathan, S. Periyasamy, S. Kandasamy, *Studia UBB Chemia*, **2025,** *LXX(2),* 163-178 DOI:10.24193/subbchem.2025.2.11
17. M. Sengottian, C.D. Venkatachalam, S.R.Ravichandran, S. Sekar, *Studia UBB Chemia*, **2024**, *LXIX(1),* 17-34, DOI:10.24193/subbchem.2024.1.02
18. X. E. Qin, G. F. Deng, Y.J. Guo, H.B. Li, *International. Journal Molecular Sciences*, **2010,** *11*, 622-646
19. M. Meini, I. Cabezudo, C.E. Boschetti, D. Romanini, *Food Chem.*, **2019**, *283*, 257-264
20. F. J. Vazquez-Armenta, B. A. Silva-Espinoza, M. R. Cruz-Valenzuela, G. A. Gonzalez-Aguilar, F. Nazzaro, F. Fratianni, J. F. Ayala-Zavala, *Journal of Adhesion Science and Technology*, **2017**, DOI: 10.1080/01694243.2017.1387093
21. A.Bondarev, S. Cuc, D. Bomboș, I. Perhaiță, D. Bomboș, *Studia UBB Chemia*, **2023**, *LXVIII(2)*, 73-84, DOI:10.24193/subbchem.2023.2.05
22. A.C. Joe, I. Onuțu, D. Bomboș, G. Vasilievici, A. Baioun, L. Silaghi-Dumitrescu, Ioan Petean, *Studia UBB Chemia*, **2025**, *LXX(2),* 129-147, DOI:10.24193/subbchem.2025.2.09
23. P. J. P. Espitia, N. de F. F. Soares, J. S. dos Reis Coimbra, N. J. de Andrade, R. S. Cruz, E. A. A. Medeiros, *Food and Bioprocess Technology*, **2012**, *5(5),* 1447–1464
24. J. Miao, W. Peng, G. Liu, Y. Chen, F. Chen, Y. Cao, *Food Control*, **2015**, *56*, 53–56
25. S. Jafarzadeh, M. Hadidi, M. Forough, A.M. Nafchi, A. Mousavi Khaneghah, *Crit. Rev. Food Sci. Nutr.* **2022**, https://doi.org/10.1080/10408398.2022.2031099
26. F. Garavand, M. Rouhi, S. Jafarzadeh, D. Khodaei, I. Cacciotti, M. Zargar, S.H. Razavi, *Front. Nutr*. **2022**, *9*, 880520
27. J. Garcia-Lomillo, M.L. González-SanJosé, L.H. Skibsted, S. Jongberg, *Food Bioproc Technol.,* **2016** *9(3),* 532–542
28. J. Gabaston, C. Leborgne, J. Valls, E. Renouf, T. Richard, P. Waffo-Teguo, J. M. Merillon, *Industrial Crops and Products*, **2018**, *126*, 272–279
29. K. Huang, Y. Wang, *Curr. Opin. Food Sci.*, **2022**, *43*, 7–17, https://doi.org/10.1016/j.cofs.2021.09.003
30. S. A. Salazar, N. Gamez-Meza, L. Medina-Juàrez, H. Soto-Valdez, P. Cerruti, *ACS Sustain. Chem. Eng.*, **2014**, *2(6)*, 1534–1542
31. Moldovan, S. Cuc, D. Prodan, M. Rusu, D. Popa, I. Petean, D. Bomboş, O. Nemes; *Polymers*; **2023** *15*, 2855
32. Trifoi, T. Gherman, O. Blajan, M. Velnazarov, R. Doukeh, Rev.Chim. (Bucharest), **2019,** *70, (12*), 4133
33. M. Lucarini, A. Durazzo, J. Kiefer, A. Santini, G. Lombardi-Boccia, E. B. Souto, A. Romani, A. Lampe, S. F. Nicoli, P. Gabrielli, N. Bevilacqua, M. Campo, M. Morassut, F. Cecchini, Foods, 2020, 9(1), https://doi.org/10.3390/foods9010010

34. Y. Gao, J. U. Fangel, W. G. T. Willats, M. A. Vivier, J. P. Moore, Carbohydrate Polymers, 2015, 133, 567–577. https://doi.org/10.1016/j.carbpol.2015.07.026.
35. J. A. Heredia-Guerrero, J. J. Benítez, E. Domínguez, I. S. Bayer, R. Cingolani, A. Athanassiou, A. Heredia, Frontiers in Plant Science, 2014, 5, 1–14, https://doi.org/10.3389/fpls.2014.00305.
36. S.E. Avram, L.B. Tudoran, C. Cuc, B. Borodi, B.V. Birle, I. Petean, *J. Compos. Sci.,* **2024**, 8, 542. https://doi.org/10.3390/jcs8120542
37. S.E. Avram, L. Barbu Tudoran, C. Cuc, G. Borodi, B.V. Birle, I. Petean, *Sustainability*, **2024**, 16, 1123. https://doi.org/10.3390/su16031123
38. S.E. Avram, L.B.; Tudoran, G.; Borodi, I.; Petean, *Appl. Sci.* **2025**, *15*, 6445. https://doi.org/10.3390/app15126445
39. G. Mugnaini, M. Bonini, L. Gentile, O. Panza, M.A. Del Nobile, A. Conte, R. Esposito, G. D'Errico, F. Moccia, L. Panzella, *Journal of Food Engineering*, **2024**, 361, 111716. https://doi.org/10.1016/j.jfoodeng.2023.111716
40. C. Corrêa de Souza Coelho, R.B.S. Silva, C.W.P. Carvalho, A.L. Rossi, J.A. Teixeira, O. Freitas-Silva, L.M.C. Cabral, *International Journal of Biological Macromolecules*, **2020**, 159, 1048-1061. https://doi.org/10.1016/j.ijbiomac.2020.05.046.
41. Petean, A. Pețan, H. Pop, S.E. Avram, L.B. Tudoran, G. Borodi, *Journal of Archaeological Science: Reports*, **2025**, 67, 105424. https://doi.org/10.1016/j.jasrep.2025.105424
42. S.E. Avram, L.B. Tudoran, G. Borodi, M.R. Filip, I. Ciotlaus, I. Petean, *Sustainability*, **2025**, 17, 2906. https://doi.org/10.3390/su17072906
43. S.E. Avram, L. Barbu Tudoran, C. Cuc, G. Borodi, B.V. Birle, I. Petean, *J. Compos. Sci.*, **2024**, 8, 219. https://doi.org/10.3390/jcs8060219
44. S.E. Avram,B.V. Birle, C. Cosma, L.B. Tudoran, M. Moldovan, S. Cuc, G. Borodi, I. Petean, *Materials,* **2025**, 18, 1715. https://doi.org/10.3390/ma18081715
45. Q. Tan, W. Zhang, C. Lai, X. Zhi, L. Xia, F. Meng, S. Zhao, *Journal of Membrane Science*, **2025**, 735, 124501. https://doi.org/10.1016/j.memsci.2025.124501
46. B. Bahramian, R. Abedi-Firoozjah, A. Ebrahimi, M. Tavassoli, A. Ehsani, M. Naebe, *Trends in Food Science & Technology*, **2024**, 154, 104761. https://doi.org/10.1016/j.tifs.2024.104761
47. H. Wu, T. Li, L. Peng, J. Wang, Y. Lei, S. Li, Q. Li, X. Yuan, M. Zhou, Z. Zhang, *Food Hydrocolloids*, **2023**, 139, 108509. https://doi.org/10.1016/j.foodhyd.2023.108509
48. T. Fu, Y. Feng, S. Zhang, Y. Sheng, C. Wang, *Food Chemistry: X,* **2025**, 25, 102182. https://doi.org/10.1016/j.fochx.2025.102182